ChemComm

RSC Publishing

COMMUNICATION

View Article Online
View Journal | View Issue

Bioactive glass nanoparticles obtained through sol–gel chemistry†

Anna Lukowiak,*[abc] Jonathan Lao,[d] Josephine Lacroix[d] and Jean-Marie Nedelec*[ab]

Cite this: *Chem. Commun.*, 2013, **49**, 6620

Received 14th March 2013, Accepted 3rd June 2013

DOI: 10.1039/c3cc00003f

www.rsc.org/chemcomm

Different sol–gel strategies based on the Stöber method are proposed enabling preparation of nanoparticles of SiO_2–CaO bioactive glass with different size, narrow size distribution and good dispersion capability. Eu^{3+}-doped glass nanoparticles with luminescent properties can also be obtained.

The sol–gel processing in fabrication of bioactive gel–glass materials was reported for the first time in 1991.[1] As compared to conventional materials obtained by the melt-quenching route (*e.g.* Bioglass®), these glasses often demonstrate higher bioactivity with higher SiO_2 limits, beyond which the powders lose their bioactive properties (up to 90% of SiO_2 instead of 60% required in Bioglass®). Moreover, the simplified binary SiO_2–CaO system obtained by the sol–gel method can be as bioactive as the quaternary system of 45S5 Bioglass®.[2] In general, this process leads to the formation of samples with high surface area rich in silanol groups that increases the degradation rate and promotes the formation of the Hydroxy Carbonate Apatite (HCA) layer.[3]

Nowadays, great interest is shown in the synthesis of bioactive glass at the nanoscale level. The nanosized powders can be used in scaffolds[4] or other nanocomposites[5] and form bioactive coatings.[6] It was shown that the nanocomposites exhibit better bioactivity and higher mechanical stability as compared to the similar microcomposites.[7] The reduced size of the particles is important for their possible direct applications in the body in the injectable systems. The bioactivity is strongly dependent on the particle size and increases with the decrease in the particle diameter that promotes the biomineralization process, increases protein adhesion, enhances osteoblast proliferation or differentiation, and engenders the anti-microbial and anti-inflammatory properties.[8]

The sol–gel procedure used for the synthesis of spherical glass nanoparticles is usually based on the modified Stöber method[9] with a two step process: the precursors are first hydrolyzed to sol under acidic conditions and then condensed to gel particles in alkaline solution.[10] Other routes have also been developed such as reactions with the addition of organic compounds (*e.g.* polyethylene glycol,[8a] Boltorn™ polymer,[11] cetrimonium bromide[12] or polystyrene beads[13]) and in water in oil microemulsion systems.[14] The described glass spheres had diameter in the range of 20–700 nm depending on the preparation method where the important parameters are temperature, pH, and composition of the reaction mixture.[10c,d,15]

In spite of the simplicity of the sol–gel method, producing spherical and monodisperse bioactive glass nanoparticles is not trivial.[16] The problems that occur after these syntheses are size irregularity, polydispersity, and agglomeration of the particles.[4c,10d,11,14c,15b,17] Also in a lot of studies, chemical analysis has not been performed questioning the chemical homogeneity of the obtained particles. Therefore, the investigation into the preparation and biological properties of the monodispersed particles in the nanometer size range is a matter of considerable importance. Herein, we present the possibility of application of the sol–gel method in preparation of spherical nanoparticles of SiO_2–CaO with different particle size distribution. In order to extend the range of possible applications of high-surface bioactive glasses, the first attempt to produce and characterize luminescent Eu^{3+}-doped nanoparticles is also described.‡

In all the performed experiments, the amount of substrates used for synthesis was calculated to obtain B75 glass, which means that the composition of $75SiO_2$–25CaO is in wt% (Table S1, ESI†). The amorphous systems have been obtained (Fig. S1, ESI†). The Standard Stöber Method (SSM), widely applied for the synthesis of monodispersed silica spheres, seems to fail in fabrication of similar silica–calcia particles. As a result of the hydrolysis of tetraethyl orthosilicate (TEOS) catalyzed with ammonia solution in the presence of calcium nitrate (CN), very fine and highly agglomerated powder was obtained with only some spherical particles that were seen on the SEM

---

[a] Clermont Université, ENSCCF, ICCF, BP10448, 63000 Clermont-Ferrand, France. E-mail: J-Marie.Nedelec@ensccf.fr
[b] CNRS, UMR 6296, ICCF, 63171 Aubière, France
[c] Institute of Low Temperature and Structure Research, PAS, Okolna 2, 50-422 Wroclaw, Poland. E-mail: A.Lukowiak@int.pan.wroc.pl; Fax: +48 713441029; Tel: +48 713954159
[d] Clermont Université, Université Blaise Pascal, CNRS/IN2P3, Laboratoire de Physique Corpusculaire, BP 10448, 63000 Clermont-Ferrand, France

† Electronic supplementary information (ESI) available: Experimental details; diffraction patterns of the MSM1 sample; the SEM micrograph of the SSM sample; and the SEM micrograph, particle size distribution, and EDS analysis of the Eu^{3+}-doped sample. See DOI: 10.1039/c3cc00003f

micrograph (∅ = 350 nm, Fig. S2, ESI†). Good results in ammonia catalyzed reaction have been previously reported but only when some additional organic compounds were used during the syntheses.[11,12]

Much better results can be achieved using the Modified Stöber Method (MSM). In this two-step procedure, TEOS was hydrolyzed first under acidic conditions, and afterwards condensed to gel particles in alkaline solution. The factors such as pH, volume of solvents or the ratio of reagents influence the chemical process of hydrolysis and polycondensation, determining the final size of the sol–gel-derived particles. The two modified Stöber methods performed in this study (MSM1 and MSM2) differ mainly in the amount of ammonia solution and water used for the synthesis (Table S1, ESI†) as well as in the step of adding calcium nitrate to the reaction mixture. In both cases, the condensation reactions occurred very fast after the addition of prehydrolysed TEOS to the ammonia solution, so the gelation time was significantly reduced as compared to the conventional sol–gel process (a few minutes instead of a few days). One can note the difference in the diameters of the obtained colloidal particles. MSM1 resulted in spheres with the average diameter of about 90 nm (Fig. 1(a) and 2(a)) whereas MSM2 gave bigger particles with the average diameter of 275 nm (Fig. 1(b)). Higher quantity of water (and a lower amount of ethanol) and lower pH during synthesis in the second case are responsible for this effect. Due to the low polarity of ethanol in comparison with water, addition of ethanol to the reaction mixture reduces the rate of hydrolysis in alkoxides and the colloid growth during the polycondensation process. Therefore, smaller glass particles are observed. In Fig. 1(d), the size distribution determined from the micrographs is presented. In the case of MSM2, the size of most of the particles is in the narrow range between 270 and 320 nm but also much smaller spheres can be seen. Therefore, the standard deviation index (SDI) calculated for the size of this powder was quite high (see Table 1). On the TEM image (Fig. 2(a)), the rough surface of these spheres is observed.

Table 1 Composition, average diameter, and specific surface area of glass particles

Sample	CaO wt%	$D_{\text{micrographs}}$ (SDI [a]) nm	D_{DLS} (PDI [b]) nm	S_{BET} m^2 g^{-1}
SSM	28	Rare spheres ≈ 350	>7000	80
MSM1	11	92 (31)	147 (0.088)	33
MSM1′	24	86 (34)	156 (0.160)	35
MSM2	19	275 (47)	358 (0.064)	15
MEM	24	92 (7)	146 (0.142)	36
Eu:MSM1	28	96 (30)	167 (0.104)	—

[a] SDI – Standard deviation index. [b] PDI – Polydispersity index.

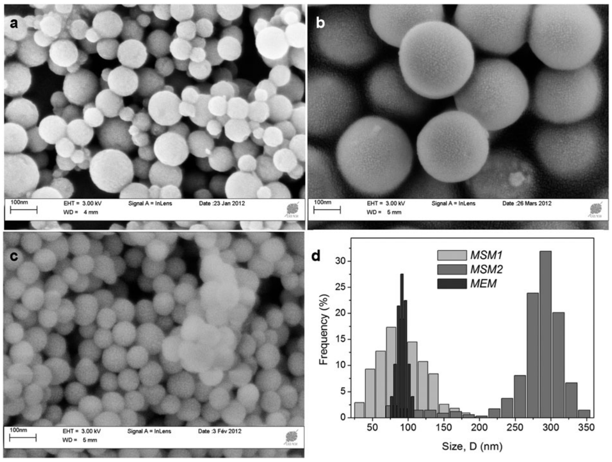

Fig. 1 SEM images of MSM1 (a), MSM2 (b), and MEM (c) samples (the scale bar is 100 nm) with size distribution of glass particles determined from micrographs (d).

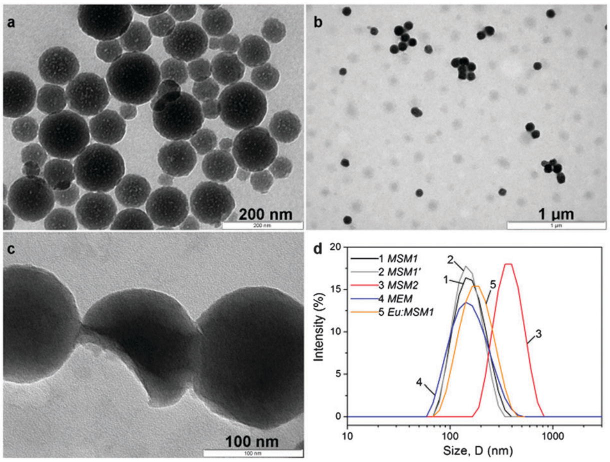

Fig. 2 TEM images of MSM1 (a) and MEM (b and c) samples with size distribution of glass particles determined by DLS (d).

The final composition of the glass may be different from the designed one. Therefore, the ratio of the oxides has been determined by energy dispersive X-ray analysis (EDS, Table 1). The compositions of nanoglasses were different from the content of the designed oxides ($75SiO_2$–25CaO) and resulted to be 11% and 19% of CaO for MSM1 and MSM2 samples, respectively. Some quantity of Ca^{2+} ions has not been incorporated into the matrix and has been removed during washing of the powders after synthesis. The incorporation of the Ca^{2+} ions was much higher when CN was added to the sol at the beginning of the synthesis (MSM2). However, a similar procedure applied in the MSM1 method has not resulted in spherical particles. To increase the amount of calcium oxide in the MSM1 sample, the following experiment was performed. The initial quantity of Ca^{2+} was increased up to 35% (MSM1′) and for this sample the final average content of CaO resulted to be 24%. Thus to obtain B75 glass, a higher amount of CN had to be used.

The Stöber method applied in the reverse MicroEmulsion (MEM) system allowed us to fabricate glass particles without the hydrolysis of TEOS under acidic conditions. The time needed for hydrolysis and condensation reactions is longer than that required in previous routes but smaller particles can be obtained (Fig. 1(c)). The average diameter of spheres estimated from the micrographs was equal to 92 nm. The micrographs indicate good monodispersity of the particles' size (Fig. 1(d)). The standard deviation index was equal to 7 and was much lower than for the MSM1 sample (SDI = 31) that had the same average size of the spheres. The TEM picture (Fig. 2(b)) confirms good dispersion of the powder in the ethanol solution. The glass seems to be formed as hollow spheres (Fig. 2(c)) which is in agreement with the previous report concerning silica particles obtained by the microemulsion technique.[18] The composition of the obtained glass (24% CaO) was almost consistent with the designed one (25%), so it was not greatly affected during the synthesis. The disadvantages of this procedure are the small amount of powder obtained as a result of the synthesis, the necessity of using organic solvents (*e.g.* cyclohexane) and the multistep washing

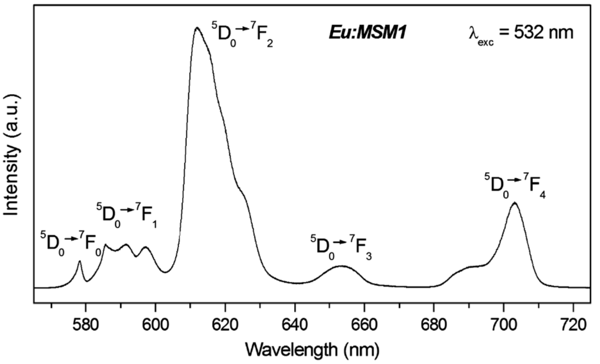

Fig. 3 Emission spectrum of the MSM1 sample doped with Eu^{3+}.

procedure needed to remove the surfactant. In contrast, the MSM methods are faster and are based on the common solvents that can be easily removed after the synthesis.

The average sizes of all the particles measured using the dynamic light scattering (DLS) technique (Fig. 2(d)) were higher than the results obtained from micrographs (Table 1) probably due to the partial aggregation. The diameters of MSM1 and MEM samples were around 150 nm. This value was higher for MSM2 particles and was equal to 360 nm. For SSM synthesis, the main distribution was bimodal with particle diameters of 300 nm (secondary mode) and 10 μm (primary mode) corresponding to aggregates (data not shown).

The specific surface area obtained for spherical particles of glass (Table 1) was the highest for MEM powder (36 $m^2\ g^{-1}$) and the lowest for bigger particles of the MSM2 sample (15 $m^2\ g^{-1}$). These values are in accordance with the result reported by Labbaf *et al.* for B86 glass with the average diameter of 250 nm and S_{BET} = 28 $m^2\ g^{-1}$.[11] A higher specific surface area (80 $m^2\ g^{-1}$) was registered in this study for the very small but agglomerated SSM particles.

The MSM1 method was used to prepare the Eu^{3+}-doped sample (Eu:MSM1) with the final composition of $70SiO_2$–28CaO–$2Eu_2O_3$. The particle size and distribution were similar to those of the undoped MSM1 sample (see Table 1, Fig. 2(d), and Fig. S3 ESI†). Under excitation at 532 nm ($^7F_1 \rightarrow {}^5D_1$), the characteristic emission spectrum of Eu^{3+} ions in glass was registered with the bands assigned to the transitions from the excited $^5D_0$ state to the ^7F_J ground state levels (Fig. 3). The bright red emission is observed mainly as a result of the most intense $^5D_0 \rightarrow {}^7F_2$ transition (615 nm). Due to the properties of europium ions as optical probes of the local structure, the detailed studies on the crystallization in the glass hosts could be further performed.[19] Moreover, Eu^{3+}-doped particles show the potential to be tracked or monitored by the luminescence that could be useful for instance in drug delivery systems.

In summary, the different modifications of the sol–gel method enabled preparation of spherical particles of SiO_2–CaO binary glass in the nano- and submicrometer size range with controlled composition and morphology. In comparison to previous reports concerning bioactive glass particles prepared by the sol–gel technique, the reported samples have a similar or slightly bigger average diameter but are less aggregated and present narrow size distribution. The high specific surface area of bioactive nanoglasses should promote faster biodegradation of the material which means fast release of the ions into the body fluids providing more nucleation sites for apatite nanocrystals. At the same time, higher protein adsorption is expected. These processes can increase significantly the bioactivity of the sol–gel-derived particles.[5c] Therefore, they are an attractive alternative to commercial Bioglass® microparticles giving new perspectives for glasses as third-generation biomaterials for tissue regeneration.

Notes and references

‡ Four different routes have been optimized for the synthesis of particles. The first one was based on the standard Stöber method (*SSM method*).[9] In the next two (MSM1 and MSM2 *methods*), the procedure was modified by performing the prehydrolysis of TEOS in acidic solution that was further added to ammonia solution. Calcium nitrate was added at the beginning of the synthesis (MSM2) or later, upon stirring the mixture under basic conditions (MSM1). An attempt has also been made to use water in an oil microemulsion system (*MEM method*) for the synthesis of particles in the presence of NH_4OH. The synthesis details and apparatus used for sample characterization can be found in ESI.†

1 R. Li, A. E. Clark and L. L. Hench, *J. Appl. Biomater.*, 1991, **2**, 231.
2 (*a*) P. Saravanapavan and L. L. Hench, *J. Biomed. Mater. Res.*, 2000, **54**, 608; (*b*) P. Saravanapavan, J. R. Jones, R. S. Pryce and L. L. Hench, *J. Biomed. Mater. Res., Part A*, 2003, **66**, 110.
3 L. L. Hench, *J. Biomed. Mater. Res.*, 1998, **41**, 511.
4 (*a*) M. Peter, P. T. S. Kumar, N. S. Binulal, S. V. Nair, H. Tamura and R. Jayakumar, *Carbohydr. Polym.*, 2009, **78**, 926; (*b*) S. I. Roohani-Esfahani, S. Nouri-Khorasani, Z. F. Lu, R. C. Appleyard and H. Zreiqat, *Acta Biomater.*, 2011, **7**, 1307; (*c*) M. Mozafari, M. Rabiee, M. Azami and S. Maleknia, *Appl. Surf. Sci.*, 2010, **257**, 1740.
5 (*a*) M. M. Sebdani and M. H. Fathi, *J. Alloys Compd.*, 2011, **509**, 2273; (*b*) M. Boguń, *Fibres Text. East. Eur.*, 2010, **18**, 11; (*c*) A. R. Boccaccini, M. Erol, W. J. Stark, D. Mohn, Z. Hong and J. F. Mano, *Compos. Sci. Technol.*, 2010, **70**, 1764.
6 (*a*) J. Liu and X. Miao, *Ceram. Int.*, 2004, **30**, 1781; (*b*) M. H. Fathi and A. Doostmohammadi, *J. Mater. Process. Technol.*, 2009, **209**, 1385.
7 (*a*) S. K. Misra, D. Mohn, T. J. Brunner, W. J. Stark, S. E. Ipsita Roy, V. Salih, J. C. Knowles and A. R. Boccaccini, *Biomaterials*, 2008, **29**, 1750; (*b*) E. Tamjid, R. Bagheri, M. Vossoughi and A. Simchi, *Mater. Sci. Eng., C*, 2011, **31**, 1526.
8 (*a*) B. Lei, X. Chen, X. Han and J. Zhou, *J. Mater. Chem.*, 2012, **22**, 16906; (*b*) R. Gupta and A. Kumar, *Biomed. Mater.*, 2008, **3**, 034005; (*c*) V. Mortazavi, M. Mehdikhani Nahrkhalaji, M. H. Fathi, S. B. Mousavi and B. Nasr Esfahani, *J. Biomed. Mater. Res., Part A*, 2010, **94**, 160.
9 W. Stöber, A. Fink and E. Bohn, *J. Colloid Interface Sci.*, 1968, **26**, 62.
10 (*a*) Z. Hong, A. Liu, L. Chen, X. Chen and X. Jing, *J. Non-Cryst. Solids*, 2009, **355**, 368; (*b*) Z. Hong, G. M. Luz, P. J. Hampel, M. Jin, A. Liu, X. Chen and J. F. Mano, *J. Biomed. Mater. Res., Part A*, 2010, **95**, 747; (*c*) A. Martinez, I. Izquierdo-Barba and M. Vallet-Regi, *Chem. Mater.*, 2000, **12**, 3080; (*d*) G. M. Luz and J. F. Mano, *Nanotechnology*, 2011, **22**, 494014.
11 S. Labbaf, O. Tsigkou, K. H. Müller, M. M. Stevens, A. E. Porter and J. R. Jones, *Biomaterials*, 2011, **32**, 1010.
12 H. S. Yun, S. H. Kim, S. Lee and I. H. Song, *Mater. Lett.*, 2010, **64**, 1850.
13 G. S. Pappas, P. Bilalis and G. C. Kordas, *Mater. Lett.*, 2012, **67**, 273.
14 (*a*) N. R. Zhao, Y. J. Wang, X. F. Chen, Y. X. Yang, K. Wei and G. Wu, *Key Eng. Mater.*, 2005, **288–289**, 179; (*b*) G. S. Pappas, P. Liatsi, I. A. Kartsonakis, I. Danilidis and G. Kordas, *J. Non-Cryst. Solids*, 2008, **354**, 755; (*c*) J. R. J. Delben, K. Pereira, S. L. Oliveira, L. D. S. Alencar, A. C. Hernandes and A. A. S. T. Delben, *J. Non-Cryst. Solids*, 2013, **361**, 119.
15 (*a*) S. I. Roohani-Esfahani, S. Nouri-Khorasani, Z. F. Lu, M. H. Fathi, M. Razavi, R. C. Appleyard and H. Zreiqat, *Mater. Sci. Eng., C*, 2012, **32**, 830; (*b*) W. Xia and J. Chang, *Mater. Lett.*, 2007, **61**, 3251.
16 J. R. Jones, *Acta Biomater.*, 2013, **9**, 4457.
17 (*a*) Y. F. Goh, A. Z. Alshemary, M. Akram, M. R. A. Kadir and R. Hussain, *Mater. Chem. Phys.*, 2013, **137**, 1031; (*b*) J. R. J. Delben, O. M. Pimentel, M. B. Coelho, P. D. Candelorio, L. N. Furini, F. A. dos Santos, F. S. de Vicente and A. A. S. T. Delben, *J. Therm. Anal. Calorim.*, 2009, **97**, 433; (*c*) A. M. El-Kady, A. F. Ali, R. A. Rizk and M. M. Ahmed, *Ceram. Int.*, 2012, **38**, 177; (*d*) N. Nabian, M. Jahanshahi and S. M. Rabiee, *J. Mol. Struct.*, 2011, **998**, 37; (*e*) X. Chen, C. Guo and N. Zhao, *Appl. Surf. Sci.*, 2008, **255**, 466; (*f*) A. A. R. de Oliveira, D. A. de Souza, L. L. S. Dias, S. M. de Carvalho, H. S. Mansur and M. de Magalhaes Pereira, *Biomed. Mater.*, 2013, **8**, 025011.
18 J. H. Park, C. Oh, S. I. Shin, S. K. Moon and S. G. Oh, *J. Colloid Interface Sci.*, 2003, **266**, 107.
19 J. K. Krebs and J. M. Brownstein, *J. Lumin.*, 2007, **124**, 257.